

# Reports

## The Melting Curve of Iron to 250 Gigapascals: A Constraint on the Temperature at Earth's Center

QUENTIN WILLIAMS, RAYMOND JEANLOZ, JAY BASS, BOB SVENDSEN,  
THOMAS J. AHRENS

The melting curve of iron, the primary constituent of Earth's core, has been measured to pressures of 250 gigapascals with a combination of static and dynamic techniques. The melting temperature of iron at the pressure of the core-mantle boundary (136 gigapascals) is  $4800 \pm 200$  K, whereas at the inner core-outer core boundary (330 gigapascals), it is  $7600 \pm 500$  K. Corrected for melting point depression resulting from the presence of impurities, a melting temperature for iron-rich alloy of  $6600$  K at the inner core-outer core boundary and a maximum temperature of  $6900$  K at Earth's center are inferred. This latter value is the first experimental upper bound on the temperature at Earth's center, and these results imply that the temperature of the lower mantle is significantly less than that of the outer core.

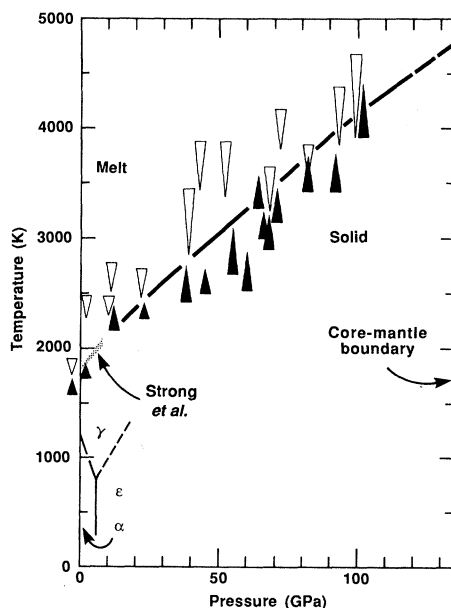
IRON IS CONSIDERED TO BE THE DOMINANT component in both the liquid outer core and the solid inner core of Earth; thus, the change in the melting temperature of iron with pressure is of considerable theoretical and experimental interest (1, 2). Such a melting curve would provide a critical upper bound on the geotherm (the temperature as a function of depth) through the core. When corrected for the melting point depression resulting from the presence of impurities, the melting curve of iron-rich alloy represents a lower limit for the possible temperature distribution through the liquid outer core (1, 3). The melting curve also gives an absolute upper limit on the temperature at the inner core-outer core boundary (4, 5). As the inner core is likely to be nearly isothermal, the temperature at the inner core boundary may be taken as close to that at the center of Earth (6). Therefore, an experimentally determined melting curve of iron provides vital constraints on the temperature distribution through the 55% of Earth's radius spanned by the core.

Despite the applications of such data to theories of Earth's evolution, thermal history, and geomagnetic dynamo, it is only

**Fig. 1.** Bounds on the melting curve of iron from static experiments as a function of pressure. Solid triangles represent the highest temperature measured on solid iron samples at a given pressure, and open triangles indicate the lowest temperature of liquid samples. Lengths of symbols reflect the standard deviation in temperature from the relevant spectral fit. The low-pressure melting curve of Strong *et al.* (2) is also shown, along with the phase equilibria of the known iron crystalline phases:  $\alpha$  represents the body-centered cubic structure,  $\epsilon$  the hexagonal close-packed structure, and  $\gamma$  the face-centered cubic structure (13).

with recent advances in static high-pressure technology and in the measurement of temperature under shock loading that the melting behavior of iron can be quantitatively measured at the conditions of Earth's core. Indeed, previous experimental determinations of the melting curve of iron under static conditions were limited to the pressure range below 20 GPa, corresponding to a depth of 600 km in Earth. Sound-speed measurements on shocked iron indicate that iron melts at 243 GPa under shock loading, but the temperature in these experiments could only be calculated with assumed values of thermodynamic parameters (5).

We have measured melting temperatures of iron (i) with a laser-heated diamond cell



to pressures in excess of 100 GPa (7) and (ii) under shock loading to determine the melting point at  $\sim 250$  GPa. In the static experiments, melting was established on the basis of textural criteria (8), and temperatures were determined by a spectroradiometric technique (9). Similarly, a four-color optical pyrometer was used to measure temperatures under shock conditions (10). Notably, these are both the highest pressure static data in which a metal has been observed to melt (by at least a factor of 5 in pressure), and the highest pressures at which temperatures have been measured under dynamic conditions. The results of the static experiments are plotted in Fig. 1, along with the previously known phase diagram of iron (2). These data represent a summary of nearly 500 separate experiments on approximately 15 different samples and  $\pm$  ranges quoted throughout are estimated standard deviations. At each pressure, 25 to 50 temperature measurements were made; however, only the lowest and highest temperatures observed in the liquid and solid, respectively, are plotted. Our data at low pressure agree with the lower pressure measurements of the melting point of iron (2).

Figure 2 shows both the static and dynamic data, with a smooth increase in sample temperature observed with increasing shock pressure. Although sound-velocity measurements imply that melting occurs at  $243 \pm 2$  GPa along the Hugoniot of iron (5), we find at most a small effect due to melting on this trend. This indicates a small internal energy difference between the solid and liquid phases where the Hugoniot intersects the melting curve: our data are consistent with a previously estimated decrease of only  $\sim 350$  K in the shock temperature due to melting (5).

On the basis of our determinations, the melting point of iron at the pressure of the core-mantle boundary, 136 GPa, is  $4800 \pm 200$  K. To evaluate the effect of a lighter alloying component on the melting temperature, we note that at pressures to 10 GPa in the iron-sulfur system the maximum depression in the melting point of iron attributable to added sulfur is about 800 K (11). Consistent with this observation and previous estimates (1, 3, 5, 12), we take a plausible value of 1000 K for the melting point depression of iron at core pressures. In detail, this estimate of 1000 K is subject to

Q. Williams and R. Jeanloz, Department of Geology and Geophysics, University of California, Berkeley, CA 94720.

J. Bass, Department of Geology and Geophysics, University of Illinois at Champaign-Urbana, Champaign, IL 61820.

B. Svendsen and T. J. Ahrens, Division of Geological and Planetary Sciences, California Institute of Technology, Pasadena, CA 91125.

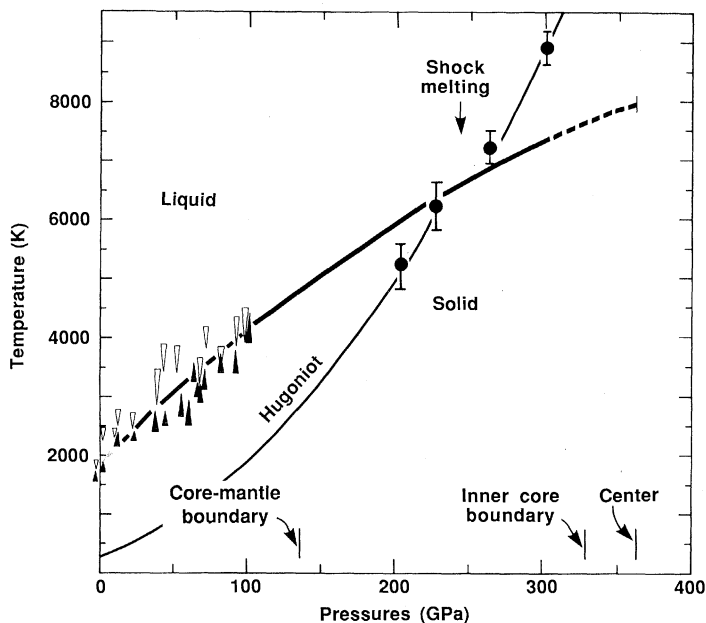


**Fig. 2.** Summary of both static and dynamic determinations of the melting temperature of iron at high pressures; circles represent measurements of Hugoniot temperatures in shock experiments, and the triangles are reproduced from Fig. 1. Shock melting pressure (243 GPa) is from Brown and McQueen (5), and our estimate of the melting curve of iron is given by the bold curve.

uncertainties in both the identity of the lighter alloying component and its chemical behavior at core pressures. We thus derive a melting temperature of 3800 K for the iron alloy at the core-mantle boundary, a value that represents a lower bound on the temperature at the top of the outer core. To maintain the outer core in its liquid state, its temperature must be higher than the melting point. Current estimates of the adiabatic thermal gradient within the convecting mantle lead to temperatures at the core-mantle boundary that are about 1000 K below this value for the melting temperature of the iron alloy outer core (12). This difference in temperatures indicates the existence of at least one thermal boundary layer across

the seismically anomalous D' layer at the base of the mantle, hence confirming that heat must be emanating from the core into the mantle (12).

Our data also provide an upper bound on the temperature at the boundary between the solid inner core and the liquid outer core: extrapolation of our data yields a melting point for iron of  $7600 \pm 500$  K at 330 GPa, and an estimated liquidus temperature of 6600 K for the iron alloy that makes up the outer core. As the inner core is thought to support an adiabatic temperature rise of at most 300 K along its radius (6), we believe that our estimate of  $6900 \pm 1000$  K represents the temperature at the center of Earth.

#### REFERENCES AND NOTES

1. F. Birch, *J. Geophys. Res.* **57**, 227 (1952); *Geophys. J. R. Astron. Soc.* **29**, 373 (1972). For a recent summary of theoretical predictions, see O. L. Anderson, *ibid.* **84**, 561 (1986).
2. L. G. Liu and W. A. Bassett, *J. Geophys. Res.* **80**, 3777 (1975); H. M. Strong *et al.*, *Metall. Trans.* **4**, 2657 (1973); K. F. Sterrett *et al.*, *J. Geophys. Res.* **70**, 1979 (1965); F. R. Boyd and J. L. England, *Carnegie Inst. Washington Yearb.* **62**, 134 (1963). A recent determination of the melting curve of iron to 43 GPa [R. Boehler, *Geophys. Res. Lett.* **13**, 1153 (1986)] with an internally heated diamond anvil cell is discrepant with our results; we attribute this to the fact that temperature gradients were not characterized in these experiments [see (9)]. The earlier results of Liu and Bassett to 20 GPa are, however, in good agreement with our data.
3. D. J. Stevenson, *Science* **214**, 611 (1981); T. J. Ahrens, *Philos. Trans. R. Soc. London Ser. A* **306**, 37 (1982). On the basis of seismological and cosmochemical constraints, the outer core is thought to be iron with 5 to 12% by weight of a lighter alloying component. The lighter component is generally inferred to be either sulfur, oxygen, silicon, or hydrogen.
4. F. Birch, *J. Geophys. Res.* **69**, 4377 (1964); A. E. Ringwood, *Geochim. J.* **11**, 111 (1977).
5. J. M. Brown and R. G. McQueen, *Geophys. Res. Lett.* **7**, 533 (1980); *J. Geophys. Res.* **91**, 7485 (1986). The difference between our measured temperatures and the estimates of these researchers suggests that electronic contributions to the specific heat of iron are small below 250 GPa.
6. The inner core is estimated to become isothermal on a time scale of the order of  $10^9$  years as a result of thermal conduction [H. S. Carslaw and J. C. Jaeger, *Conduction of Heat in Solids* (Oxford Univ. Press, Oxford, 1959), p. 55]. A relatively high value of thermal diffusivity ( $1 \times 10^{-5}$  to  $2 \times 10^{-5}$   $\text{m}^2 \text{sec}^{-1}$ ) is inferred for iron at the appropriate conditions on the basis of electrical resistivity measurements under shock loading [G. Matassov, *The Electrical Conductivity of Iron-Silicon Alloys at High Pressures and the Earth's Core*, report UCRL-52322, (Lawrence Livermore National Laboratory, Livermore, CA, 1977); R. Jeanloz, *Sci. Am.* **249**, 56 (September 1983)]. Paleomagnetic measurements imply that the inner core is likely to have been present for at least the past 2.5 billion to 3.5 billion years [R. Merrill and M. McElhinny, *The Earth's Magnetic Field* (Academic Press, New York, 1983), p. 177]. Although there may now be only a small thermal gradient in the core, the maximum isentropic temperature rise through the inner core is estimated to be about 300 K, on the basis of the data of Brown and McQueen (5).
7. An iron foil (99.99% purity) of approximate dimensions 75 by 75 by 20  $\mu\text{m}$  was surrounded by ruby ( $\text{Al}_2\text{O}_3:\text{Cr}^{3+}$ ) and compressed in a gasketed, Mao-Bell type diamond cell [H. K. Mao *et al.*, *Rev. Sci. Instrum.* **50**, 1002 (1979)]. As iron can react with diamond at high temperatures, it is necessary to prevent the foil from directly contacting either of the diamonds by using a layer of ruby to enclose the sample. Pressure was accurately profiled at 10- $\mu\text{m}$  intervals across the iron sample by use of the ruby fluorescence technique [H. K. Mao *et al.*, *J. Appl. Phys.* **49**, 3276 (1978)]; maximum pressure variations across a single sample were about 20 GPa. Because of the competing effects of stress-gradient relaxation during heating and the thermally induced increase in pressure, the pressure at high temperature was taken to be the same as that measured at 300 K prior to heating (9). Samples were heated with a continuous-wave neodymium:yttrium-aluminum-garnet laser tuned to the 00 transverse electromagnetic mode; operation in this mode provided 20 W at 1060 nm. The diameter of the laser beam (and thus, the heated region of the sample) was about 25  $\mu\text{m}$  at the focus in the sample.
8. Melting of the sample inside the diamond cell was determined to have occurred on the basis of two criteria: (i) observation of annihilation of grain boundaries and other surface-textural features present on the iron foil after thermal quenching; and (ii) observation of fluid-like motion in the sample when held at high temperature. If, on quenching, surface features on the sample were preserved, the sample was assumed to be solid. After an area of a sample had been melted, no further measurements were performed in the same region of the sample: temperatures were observed to decrease after numerous melting episodes in the same spot, and we interpret this as being due to reaction with the  $\text{Al}_2\text{O}_3$  matrix.
9. R. Jeanloz and D. L. Heinz, *J. Physique* **C8**, 83 (1984); *Proceedings of the International Congress on the Applications of Lasers and Electro-Optics*, C. Albright, Ed. (Springer-Verlag, New York, 1986), p. 239; D. L. Heinz and R. Jeanloz, in *High Pressure Research in Geophysics and Geochemistry*, M. H. Manghnani and Y. Syono, Eds. (American Geophysical Union, Washington, DC, in press). A monochromator and a photomultiplier tube are used to measure the spectrum of the light emitted by the laser-heated sample between 620 and 780 nm; the resultant spectrum is fit to a Wien gray-body function, and inverted for both average sample temperature and emissivity. The average temperature is then corrected upward to the peak sample temperature, based on both measurements of the thermal profile across the sample and previous calculations (further details will be given by Q. Williams and R. Jeanloz, in preparation).
10. Spectral radiances of shocked samples were observed at four wavelengths (450, 600, 750, and 900 nm), and fit to a Planck gray-body function. The samples were either vapor-deposited iron films (about 1  $\mu\text{m}$  thick) or thin foils (about 25  $\mu\text{m}$  thick), held on a substrate of either  $\text{Al}_2\text{O}_3$  or LiF. The  $\text{Al}_2\text{O}_3$  or LiF served as a window through which thermal radiation from the shocked sample was detected [see also G. Lyzenga and T. Ahrens, *Rev. Sci. Instrum.* **50**, 1421 (1979); *Geophys. Res. Lett.* **7**, 141 (1980); J. Bass, B. Svendsen, T. Ahrens, in *High Pressure Research in Geophysics and Geochemistry*, M. H. Manghnani and Y. Syono, Eds. (American Geophysical Union, Washington, DC, in press)].
11. T. M. Üsselman, *Am. J. Sci.* **275**, 278 (1975); S. Urakawa, M. Kato, M. Kumazawa, in *High Pressure Research in Geophysics and Geochemistry*, M. H. Manghnani and Y. Syono, Eds. (American Geophysical Union, Washington, DC, in press).
12. R. Jeanloz and F. Richter, *J. Geophys. Res.* **84**, 5497 (1979); F. D. Stacey, *Phys. Earth Planet. Inter.* **15**, 341 (1977); R. Jeanloz and S. Morris, *Annu. Rev. Earth Planet. Sci.* **14**, 377 (1986); S. Spiliopoulos and F. D. Stacey, *J. Geodyn.* **1**, 61 (1984).
13. The location of the  $\epsilon$ - $\gamma$ -liquid triple point is a matter of debate (1); however, it appears from the work of Brown and McQueen (5) that it lies at pressures above 200 GPa. If the  $\epsilon$ - $\gamma$  phase boundary intersects the melting curve, the slope of the melting line must increase in accord with Schreinemakers' rule. Such an effect is not resolved in our data.
14. We are grateful to E. Knittle, D. L. Heinz, D. J. Stevenson, and J. M. Brown for helpful comments and experimental advice. Work supported by NSF and NASA, including grants EAR8313746, EAR8419259, and EAR8508969 to the California Institute of Technology. This is contribution 4425 of the Division of Geological and Planetary Sciences of the California Institute of Technology.

8 December 1986; accepted 29 January 1987